

10627
NACA TN 4285

TECH LIBRARY KAFB, NM
0066930

NATIONAL ADVISORY COMMITTEE FOR AERONAUTICS

TECHNICAL NOTE 4285

TRANSGRANULAR AND INTERGRANULAR FRACTURE

OF INGOT IRON DURING CREEP

By L. A. Shepard and W. H. Giedt

University of California
Berkeley, California



Washington

August 1958

TECHNICAL LIBRARY
AUG 1958



NATIONAL ADVISORY COMMITTEE FOR AERONAUTICS

TECHNICAL NOTE 4285

TRANSGRANULAR AND INTERGRANULAR FRACTURE

OF INGOT IRON DURING CREEP

By L. A. Shepard and W. H. Giedt

SUMMARY

Creep tests were performed on coarse-grained ingot iron over a temperature range from 700° to 1,350° F to find whether the amount of grain-boundary sliding determined the fracture mode, either transgranular or intergranular. If the fracture mode were thus determined, it could be demonstrated that a critical stress rather than a critical temperature is the criterion for intergranular fracturing.

Transgranular fractures were obtained at temperatures below 800° F and stresses above 20,000 psi. At higher temperatures, and necessarily lower stresses, all fractures were intergranular.

Tests on gridded specimens indicated that, though appreciable grain-boundary shearing occurs at the higher temperatures, intergranular fracturing may occur without any observable grain-boundary shearing in the lower temperature range.

From a review of test results and current theory, it was concluded that a vacancy-condensation mechanism is most probably responsible for high-temperature intergranular fracturing in ingot iron.

INTRODUCTION

All engineering metals and alloys will fail intergranularly if subjected to a low stress or strain rate at high temperature. This fact, stated in essence many years ago in reference 1, has been repeatedly confirmed by numerous subsequent creep investigations. Several papers have been devoted to theoretical interpretation of this phenomenon (refs. 2 to 5). And with requirements for high-strength - high-temperature metals becoming more stringent with each passing day, the problem becomes one of extreme practical as well as theoretical significance.

At normal temperatures, metals usually fail in a ductile transgranular manner by a shearing process with local necking. Grain boundaries are extremely resistant to failure. The few isolated but important cases of grain-boundary failure have been satisfactorily established as being due to impurities in the grain boundary (e.g., small amounts of oxygen in iron) which acted as stress raisers or lowered the grain-boundary interfacial energy.

At high temperatures and low stress or strain rates, where intergranular fracturing is the rule rather than the exception, the cause is by no means as clear. It has been variously attributed to:

- (1) Impurities, either present in the metal or absorbed from the atmosphere, which diffuse to the grain-boundary region and embrittle the boundary or render the material in the boundary vicinity incapable of recovery (refs. 6 and 7)
- (2) Vacancies generated during high-temperature straining which diffuse to the grain boundaries and coalesce into grain-boundary cracks (refs. 5, 8, and 9)
- (3) Grain-boundary shearing that becomes prominent during high-temperature deformation which leads to cracking due to excessive local-strain damage in the boundary and the high stresses induced at the triple point locking the ends of each boundary (ref. 4)

A review of the literature indicates that in specific cases any of the three proposed causes may play an important role. Whether it is the basic cause for intergranular fracture or only a contributing factor is a more difficult question to answer. However, it should be emphasized that intergranular fracturing occurs in the temperature range where atomic mobility is high and all the forementioned mechanisms can act with relative facility. The temperature at which intergranular fracturing is first observed, the so-called equicohesive temperature, is often associated with the recrystallization temperature of the metal (ref. 2), though it varies considerably as a function of stress or strain rate.

Grain-boundary cracking is first noted in the third stage of creep, or at the ultimate tensile strength in a tensile test. The cracks open and spread, and the final fracture is partially or wholly intercrystalline, with visible cracks appearing also in regions considerably distant from the major fracture. In fine-grained specimens it frequently appears as though each grain had separated from its neighbor. Specimens which fracture intergranularly very often show little deformation within the grains. The two notable features of the cracks which form are:

- (1) The cracks usually appear in grain boundaries which are normal to the direction of stressing (ref. 10).

(2) The cracks are formed at the surface of the specimen. Thus, cracks found on the interior of a sectioned specimen which has been tested in air are covered with an oxide scale.

Grain-boundary fracture is usually accompanied by a decreased elongation to fracture with very little or no necking, the decrease being particularly marked at the higher temperatures where rupture strains of only a few percent are the normal case. The rupture life is also markedly lowered with the onset of intergranular fracturing. This observation has been formalized in the many constant-temperature curves of log stress against log rupture time in the creep literature as a break in the straight-line plot to a line with a more steeply descending slope with the onset of intercrystalline fracture at lower stresses. This break is often specifically determined by auxiliary microscopic observations of the fracture (ref. 11), though a range of stresses exists over which the fracture is partly transcrystalline and partly intercrystalline.

This investigation was conducted at the University of California under the sponsorship and with the financial assistance of the National Advisory Committee for Aeronautics. The authors wish to acknowledge the aid of Messrs. Leonard Levenson, Neville Daniels, John Nadau, William Masuda, and Theodore Lachelt in the design of the test equipment and the administration of test details.

THEORIES OF INTERGRANULAR FRACTURE

The three basic mechanisms mentioned as possible causes of high-temperature intergranular fracture, the embrittlement of grain boundaries by impurities, the formation of microcracks as the result of vacancy condensation at the boundary, and the opening of cracks due to grain-boundary sliding, are now considered in more detail, along with experimental observations in support of each.

Embrittlement of grain boundaries by impurities either by absorption from the test atmosphere or by diffusion from within the crystals has been proposed as the cause for intergranular fracture (ref. 6). In support of these conclusions reference 6 cites the work reported in reference 12 in which 5-percent-chromium 0.5-percent-molybdenum steel failed intergranularly with marked grain-boundary oxidation at 1,100° F, whereas the same alloy with an addition of 1.5 percent silicon to suppress oxidation failed transgranularly at both 1,100° and 1,200° F. Reference 12 also reports that grain-boundary failure in a stabilized 18-8 stainless steel was associated with excessive carbide precipitation in the boundaries. Increasing pressures of air from 5×10^{-5} millimeters of mercury to 1 atmosphere produced a growing tendency to intergranular fracture with increasing time to failure (ref. 13). This observation was interpreted

in terms of boundary embrittlement due to oxidation. References 7, 11, and 14 suggest a second role of impurity atoms in promoting intergranular fracturing. It is proposed that impurities "stiffen" the matrix of the metal grains without similarly strengthening the grain boundaries. This action not only promotes relative grain-boundary weakness but inhibits recovery of the highly stressed metal in the grain-boundary region by polygonization or boundary migration. Thus, the boundary cracks when it can no longer accommodate the localized stresses which develop in its vicinity.

Without considering the detailed mechanism, aluminum is probably the best example for demonstrating the effect of impurities. High-purity aluminum, 99.99 percent or better, does not fail intergranularly at any stress or temperature (ref. 11); this is the single exception to the general rule to be found in the literature that all metals fail intergranularly. However, 99.6 percent aluminum (ref. 15) as well as 99.3 and 98.2 percent aluminum (2S and 3S) all exhibit grain-boundary fracture at temperatures above 500° F.

The theoretical work of reference 16 on the generation of vacancies during straining and the experimental verification of the role of vacancies in diffusion from tests of the type initiated by Kirkendall has stimulated interest in a vacancy-condensation mechanism for intergranular fracturing. References 8 and 14 propose that excess vacancies generated during straining by dislocation cutting processes condense on voids, gas pockets, small cracks, or precipitated particles at or near the grain boundary to form larger holes and eventually cause fracture. Reference 8 concludes that when vacancy condensation is the cause of fracture the dimensionless product of the secondary-creep rate and the rupture time is a constant independent of creep stress or temperature.

Two types of evidence may be cited in support of this theory. The first is the grain-boundary pore formation observed in the work of references 9 and 17 during the creep of α brass which led to intergranular fracture. Pore formation occurs during dezincification of the brass, the unequal diffusion of zinc and copper resulting in an excess concentration of lattice vacancies which condense into holes (ref. 18). It is reasonable to believe that the boundary pores found during the creep of brass are due to the same factor, the effect occurring at a lower temperature during creep as a result of the enhanced diffusion rate with straining.

Reference 9 presents evidence for similar grain-boundary pore formation in low-strain-rate tests on oxygen-free high-conductivity copper and magnesium where the vacancy concentration excess is certainly lower than that of α brass. Reference 19 reports the phenomenon in transverse boundaries of an age-hardenable copper-nickel-silicon alloy in creep.

The second type of evidence is a density change measured during creep of aluminum (ref. 15). The density decreased only slightly during primary and secondary creep and then dropped sharply during tertiary creep.

4936 It is interesting to note that in the calculations of reference 8 the existence of void nuclei such as cracks in brittle particles or voids formed during working was assumed, for it was concluded that nucleation does not control void formation. Furthermore, reference 19 refers to observed boundary cavitation as "distortion cavities", which implies that a grain-boundary weakness led to their formation. Such observations suggest the third proposed mechanism, and in its simplest form, the oldest; namely, that high-temperature intergranular fracturing is the result of grain-boundary shearing, which leads to crack formation both as the result of excessive local strain damage in the boundary and because of the high stresses induced at the triple point locking the ends of each boundary.

The idea of high-temperature grain-boundary weakness causing intergranular fracturing was originally proposed in reference 1 and later crystallized in reference 2, the paper introducing the concept of the equicohesive temperature, the temperature above which the grain boundaries are less resistant to deformation than the grains. Though this theory was developed around the now discredited idea of amorphous grain-boundary cement, it continues to appear in the literature as an explanation for high-temperature fracturing characteristics (ref. 11). Disassociated from its basic idea, the equicohesive-temperature concept is simply another way of describing an observation, rather than an explanation of the cause. A more fundamental evaluation of the role of grain-boundary deformation in intergranular fracturing is necessary before the process can be assessed from this viewpoint. Such an evaluation has recently been undertaken by the work of reference 4 and, from a different vantage point, by the work to be described herein.

The workers of reference 4 approached the problem by choosing an alloy, aluminum with 20 percent zinc, which showed intergranular fracturing at 500° F with low elongation, a large amount of grain-boundary deformation, and little tendency for recovery or grain-boundary migration. All these factors would relieve the stresses developed at bent grain boundaries and triple points resulting from boundary sliding. This alloy thus possessed the properties desirable for a detailed study on the fractures resulting from the shearing of boundaries alone. The majority of the intercrystalline cracks clearly resulted from the inability of the transverse boundaries to support the stresses developed at grain triple points as the result of the sliding of diagonal boundaries (ref. 4). To a lesser extent, cracking developed because of bending stresses when strain was not transmitted across a grain boundary. The rate of propagation of the cracks to final fracture was highly dependent

on the ability of the grains to deform and relieve the stress concentrations arising from the cracks.

The present work differs from that of reference 4 in approach and emphasis rather than concept. Its thesis is based on two observations relative to the role of grain boundaries in high-temperature creep (observations (1) and (2) are from ref. 20; observation (3), from ref. 21):

(1) The creep strain resulting from grain-boundary shearing ϵ_{gb} is proportional to the total strain ϵ throughout the creep test at constant stress and temperature, that is,

$$\epsilon_{gb}/\epsilon = \text{Constant}$$

(2) As the creep stress is reduced, the ratio ϵ_{gb}/ϵ increases; that is, an increasing proportionate amount of grain-boundary sliding is observed with decreasing applied creep stresses.

(3) Above a lower limiting temperature the constant ratio ϵ_{gb}/ϵ is independent of the test temperature for tests at a given stress.

Thus, the amount of grain-boundary shearing is proportional to the total strain, this ratio being constant at any constant stress, independent of the test temperature, and increasing with decreasing stress. If grain-boundary shearing is the factor responsible for intergranular fracturing, then a critical stress, rather than a critical temperature, should be found which determines the mode of fracture, because it is with a decrease in stress that an increasing proportionate amount of grain-boundary shearing is observed. The investigation discussed herein was undertaken to test this hypothesis.

TEST MATERIAL, EQUIPMENT, AND PROCEDURE

The test series was conducted on magnetic ingot iron supplied in 1/8- by 1-inch cold-rolled strip. The nominal composition of the iron quoted by the supplier in weight percent is:

C	P	Mn	S	Si	Fe
0.015	0.005	0.028	0.025	0.003	Balance

Spectrographic analysis of a heat-treated sample showed:

Mn	Cu	Ni	Cr	Si
0.04	0.1	0.04	0.02	Not detected

The strip was cut and machined into constant-stress $4\frac{1}{4}$ inch specimens with a $1\frac{1}{4}$ - by 2-inch gage section and $1\frac{1}{4}$ -inch-radius fillets to the shoulders. All specimens were given a 2-hour heat treatment in helium at $2,300^{\circ}$ F and then slowly cooled in order to produce large ferrite grains suitable for observation of grain-boundary sliding. An average grain size of 0.5 millimeter was produced by this treatment with little duplexing.

Three additional specimens were heat-treated in high vacuum (10^{-5} mm of mercury) as a check on the effect of the helium atmosphere during grain-growth annealing. Little difference was noted in test results from the different treatments.

Tests were conducted in specially modified inert-atmosphere constant-stress creep testing units (fig. 1). The specimen and extensometer were contained within a gas-tight Inconel tube with a removable O-ring seal at the bottom and a gas-sealed cap at the top with windows on either side for reading the creep strain. In earlier tests the top cap was fastened to the upper pulling tab and moved in a water-cooled mercury seal as the specimens strained. This arrangement was later modified for simpler operation by using a soft flexible rubber bellows seal between the cap and the pulling tab and a rubber boot seal between the cap and the tube extension.

The system was flushed by blowing high-purity helium through it in such quantity as to reduce the remaining oxygen to a negligible amount by simple mixing. Thereafter the helium flow was reduced to a small constant value, which was maintained during subsequent specimen heating, testing, and cooling. Some oxidation of the specimen surfaces was observed in all cases in spite of these precautions. Attempts at gettering the oxygen remaining in the system with heated copper gauze and titanium chips did not produce a noticeable improvement.

The specimen was fastened to the pulling tabs at the top and bottom with a set of crossed-pin joints to assure axial alignment. Similar connections were used at the bottom of the lower pulling tab and at the top of the upper pulling tab.

The extensometer consisted of two sets of concentric rods and tubes clamped to either side of the specimen shoulders with locating pins $2\frac{1}{4}$ inches apart and guided at the top with frictionless ball bushings. Two dial gages with least counts of 0.001 inch were mounted to the tubes and operated by the rods to indicate extension. By simultaneously reading the two gages and averaging the results, effects of bending of the flat specimen were eliminated from the strain record. Checks on dummy specimens showed that elongations measured at the shoulders corresponded to an active gage length of 1.8 inches, and elongation values were divided by this factor to obtain engineering strain.

The Inconel tube containing the specimen and extensometer was surrounded by a three-zone electrical resistance furnace with separate variable power to each winding. The furnace was controlled by a self-balancing potentiometric controller with a Chromel-Alumel thermocouple located at specimen height between the liner and the furnace wall. Temperatures were maintained to within less than $\pm 3^{\circ}$ F of the reported values over the specimen gage length as determined from readings of two separate thermocouples mounted to the specimen shoulders and read periodically throughout the test.

A stress constant to within 1 percent of the reported value was applied to the specimen throughout the test by use of an Andrade type contoured constant-stress lever arm. The arm is designed to compensate for the reduction in area of a specimen as it elongates by decreasing the lever arm ratio and thus maintain a constant true stress. As the initial position of the lever arm is an important factor governing the applied stress in the use of this type of arm, all slack in the load system was taken up with a turnbuckle before loading. The movement of the lever arm during loading was thus essentially due to the elastic and plastic straining of the specimen.

The testing procedure was as follows. The specimen, extensometers, and upper and lower pulling tabs were assembled and inserted into the cold furnace, and the furnace was sealed against the atmosphere. High-purity helium was then blown through the sealed system in excess of the quantity calculated to reduce the retained oxygen to a few molecules per million by simple mixing. The helium flow was reduced to a low constant value maintained for the remainder of the test, and the furnace was heated to the test temperature in 6 to 12 hours. The slack was removed from the loading system, and the load applied to the lever arm. Specimen strain was read and recorded for both sides of the specimen at 15-second intervals at the start and at longer intervals as the strain rate decreased. Average values of the two readings were used in plotting strain in the creep curves.

TEST RESULTS

Results are summarized in table I for creep tests on ingot iron from 700° to 1,350° F. Secondary-creep rate and fracture time are shown as functions of stress in figures 2 and 3, respectively, for the significant 700° to 800° F temperature range where both transgranular and intergranular fractures were observed.

Specimen letter and number designations noted to the left in table I indicate the strip and section, respectively, from which each specimen was machined. Fifteen specimens were machined from each strip. Specimens of the T series were heated in vacuum in the initial grain-growth treatment. Specimens of series X were machined from strip C, mechanically polished on one side, and gridded with horizontal lines 0.01 inch apart using a diffraction-grating ruling machine. These specimens were used to observe grain-boundary shearing.

The following factors served as criteria in determination of the mode of fracture, which is listed on the right in table I:

- (1) Transgranular fracture: Local necking, a smooth silky fracture, and no intergranular cracks away from the fracture
- (2) Intergranular fracture: Little tendency for necking, a pitted fracture surface, usually with the shiny surfaces of grain boundaries visible, and often with some partially separated grains present, and prominent intergranular cracks away from the fracture

Examples of both types are shown in figure 4. Mixed fractures, showing both a little necking and cracks away from the fracture, were designated as T(M) or I(M), the designation being somewhat arbitrary. However, it should be noted that all fractures except those marked T showed some tendency toward the intergranular fracture mode.

DISCUSSION

The test conditions outlined in table I cover the temperature range from 1,350° F, slightly above the eutectoid temperature, to 700° F and the corresponding stress range from 2,500 to 27,500 psi.

Initial tests were conducted at temperatures above one-half the absolute melting temperature of iron, 1,150° to 1,350° F, in the hope that data on transgranular and intergranular fracturing could be correlated on the basis of the temperature-modified time parameter previously used successfully for the correlation of high-temperature creep, grain-boundary shearing, and fracture data (ref. 22). For the majority of metals, to which this correlation can be applied, it has been shown that fracture

strains at any one stress are independent of temperature, and times to failure are related through the equation

$$\epsilon_{fr\sigma} = K = f_{\sigma} \left(t_{fr} e^{-\Delta H/RT} \right) \quad (1)$$

where

$\epsilon_{fr\sigma}$	fracture strain at stress σ
f_{σ}	function representing form of creep curve under stress σ
t_{fr}	fracture time
ΔH	activation energy for creep and self-diffusion, 78,000 cal/mole for ingot iron
R	gas constant
T	absolute temperature

Because both the amount of grain-boundary shearing and the fracture strain can be correlated through this parameter, the method suggested itself as a good approach to the delineation of the effect of stress upon the fracture mode, as mentioned in the INTRODUCTION.

However, two factors militated against the application of this approach to the problem of intergranular fracturing in ingot iron. First, all fractures at temperatures above one-half the absolute melting temperature were intergranular, even at the highest stresses that could reasonably be applied, as is noted in table I. Second, fracturing in ingot iron, both intergranular and transgranular, occurs quite abruptly during secondary creep, the normal creep curve exhibiting little or no tertiary stage. This effect can be seen in the creep curves of figure 5, which are typical also of the higher temperature results.

If the mechanism proposed in the INTRODUCTION controlled intergranular fracturing in ingot iron and the relation given in equation (1) applied, fracture strains would delineate the intergranular and transgranular mode. However, because of the abruptness of fracture alone, fracture strains proved a poor criterion.

Transgranular fracturing was first observed upon extension of test conditions to the 700° to 800° F temperature range and to stresses above 20,000 psi. No transgranular fracturing occurred above 800° F, and from the test results, it seems reasonable to assume that even at extremely low strain rates intergranular fracturing will not occur at temperatures much below 700° F. This observation is in substantial agreement with the work of reference 7.

In this respect, ingot iron appears to differ from most metals, the general rule being a rather broad temperature range in which either transgranular or intergranular fracturing may be obtained. For example, 2S aluminum exhibits both fracture modes, depending upon the creep stress, from 500° to 1,100° F (ref. 11).

Fracture strains were roughly half the normal values appearing in the literature for ingot iron, most probably because of the large grain size used in this investigation. Room-temperature tests to failure exhibited about 28-percent elongation, and creep strains varied from 3 percent at 1,150° F to 33 percent at 750° F. With the exception of the relatively high ductility observed at 1,350° F, the fracture strains ran less than 15 percent above 800° F and decreased with decreasing creep stresses.

It is a peculiar fact that the percent elongation is not related to the mode of fracture in ingot iron. This, as previously noted, is apparently due to the abrupt nature of the fracturing during secondary creep and the lack of a tertiary stage. Examples of pairs of specimens which fractured both transgranularly and intergranularly at the same stress and temperature selected from table I and shown in table II bear out this statement.

In the 700° to 800° F temperature range, where both modes of fracture were observed, transgranular fracture strains ranged from 15.7 to 36.1 percent, and intergranular fracture strains from 15.0 to 30.5 percent.

It is suggested in reference 23 that, since the percent elongation values are measured on the fractured specimen and include the local deformation effects just preceding fracture, a better strain measurement for differentiating fracture characteristics is the strain at the end of secondary creep. Values for ϵ_{end} in table II clearly demonstrate that this criterion also fails for ingot iron.

The secondary-creep rate was in general lower and the fracture times were greater for specimens that fracture transgranularly, as is noted in tables I and II. This observation is in agreement with the findings on other metals.

It is noted in reference 11 that the product of the secondary-creep rate and the fracture time is fairly constant over a wide range of stresses and temperatures. This relation is also derived in reference 8 in the vacancy-condensation theory for fracture. The plot of log secondary-creep rate against log fracture time in figure 6 for the 700° to 800° F data for ingot iron shows quite good agreement on the basis of this correlation.

With the exception of those specimens in the 900° to 1,150° F temperature range which showed relatively low ductility, specimens which fractured intergranularly seemed to be able to withstand a large amount of grain deformation without boundary cracking, as evidenced by the prominent "orange peel" observable on the surface. Cracks when they appeared opened from the surface mostly in transverse boundaries. Failures frequently resulted from cracks that opened at one edge of the specimen width and forced a bending of the specimen to maintain stress alignment and an eventual crosswise tearing at this point of high deformation. This observation is not meant to explain the failure of ingot iron to show tertiary creep, for such was the case even when prominent necking and completely transgranular fracturing occurred.

The uncracked grain boundaries in metallographic samples taken from fractured specimens showed no unusual appearance. Boundaries which had fractured were attacked by the etchant to a slightly greater extent than the rest of the specimen. It is believed that this was due to a small amount of oxidation which occurred at the new surfaces after the cracks opened, rather than to some phenomenon leading to the cracks. This belief is borne out in the work of references 7 and 12 which showed intergranular fracturing in ingot iron tested in vacuum and hydrogen, respectively, which demonstrates that oxidation is not an important factor.

Recrystallization at the grain boundaries, an effect ascribed by some authors to cause intergranular fracturing, was observed in only one case, in a specimen at the highest temperature, 1,350° F, in which small new grains were formed at the fracture surface. It is most probable that this recrystallization occurred after fracturing as the result of the combined effects of high local straining and high temperature.

In the high-temperature tests using gridded specimens, some grain-boundary shearing was observed, as is shown in the center of figure 7. However, this gross grain-boundary displacement appeared to be quite localized, and observation of the over-all area indicated relatively few examples of grid lines sheared across grain boundaries.

Examination of specimens tested in the 700° to 800° F range where both fracture modes were obtained showed essentially no grain-boundary shearing. As can be seen in figures 8(a) and (b), the grain boundaries of specimens which fractured intergranularly underwent considerable distortion without either sliding or cracking. Furthermore, where cracks did occur, the metal interfaces separated without displacing the grid lines (fig. 8(c)).

These results may be contrasted with those for pure aluminum (fig. 8(d)) where both grain-boundary sliding and migration are prominent.

In summary, the observations on transgranular and intergranular fracturing in creep of coarse-grained ingot iron indicated:

(1) Transgranular fracturing occurs at temperatures below 800° F and stresses above 20,000 psi. At higher temperatures and lower stresses all fractures are intergranular.

(2) Fracturing occurs with little or no tertiary creep.

(3) Percent elongation is not a criterion for fracture mode.

(4) Specimens fracturing transgranularly exhibit markedly lower secondary-creep rates and greater fracture times than those fracturing intergranularly under identical test conditions. The dimensionless product of fracture time and secondary-creep rate is reasonably constant and independent of stress and temperature.

(5) Neither oxidation nor recrystallization seems to be an important factor in intergranular fracture.

(6) Intergranular fracture may occur with no preceding grain-boundary shearing.

In the light of these observations, it is clear that intergranular fracturing in ingot iron is not produced by the grain-boundary shearing mechanism proposed in the INTRODUCTION. Thus, the criterion of the intergranular fracture stress rather than the equicohesive temperature could not be tested from this series of results. This does not necessarily mean that the concept is incorrect. It does signify that, in order to satisfactorily test this hypothesis, a metal must be chosen in which grain-boundary shearing is facile and brittle second-phase particles or boundary conditions favorable to vacancy condensation are not present.

A review of the results on intergranular fracturing in ingot iron suggests that the vacancy-condensation mechanism proposed by Machlin (ref. 8) and others is most probably the responsible factor. The constancy of the product of the fracture time and the secondary-creep rate is in good agreement with Machlin's results. Furthermore, the existence of a second phase at the ferrite grain boundaries, though not observed microscopically, seems most likely from the difficulties encountered in trying to promote grain growth in this metal. These second-phase particles could be either iron sulfides (since the manganese-to-sulfur ratio in ingot iron is 1, which is generally believed to be too low to suppress the formation of iron sulfides) or oxides resulting from selective adsorption of small amounts of oxygen at the grain boundaries at the 2,300° F heat-treatment temperature. Either could act as vacancy collectors for the promotion of void formation.

This conclusion is corroborated by the very recent experimental results of reference 24 on intergranular fracturing resulting from vacancy condensation during the creep of α brass. These results show that, by removal of impurities from metal by a directional solidification process, premature intergranular fracturing was suppressed and the fracture strain was more than doubled.

The low percent elongations and abrupt fracturing tendency with little or no tertiary creep are reasonably accounted for by the large grain size. When an intergranular crack opened at a grain boundary or a single favorably oriented grain necked in a transgranular fracture, the resulting local-stress increase on the cross section promoted almost immediate failure.

CONCLUSIONS

The following conclusions were drawn from creep tests performed on ingot iron over a temperature range from 700° to 1,350° F to find whether the amount of grain-boundary sliding determines the fracture mode:

1. Intergranular fracturing in ingot iron does not occur as the result of localized grain-boundary strain damage due to intergranular shearing. However, this does not deny the possibility of this mechanism being responsible for intergranular fracture in other metals.
2. Evidence from the relation between secondary-creep rate and fracture time and from grain-growth characteristics points to vacancy condensation such as detailed by Machlin as the predominant factor promoting intergranular fracture in ingot iron.

University of California,
Berkeley, Calif., January 1, 1957.

REFERENCES

1. Rosenhain, Walter, and Ewen, Donald: Intercrystalline Cohesion in Metals. Jour. Inst. Metals, vol. 8, 1912, pp. 149-173.
2. Jeffries, Zay: Effect of Temperature, Deformation, and Grain Size on the Mechanical Properties of Metals. Trans. AIME, vol. 60, 1919, pp. 474-562; discussion, pp. 562-576.
3. Parker, E. R.: Intercrystalline Cohesion of Metals. Trans. ASM, vol. 33, 1944, pp. 150-160.
4. Chang, H. C., and Grant, Nicholas J.: Mechanism of Intercrystalline Fracture. Jour. Metals, vol. 8, no. 5, sec. 2, May 1956, pp. 544-551.

5. Crussard, C., and Friedel, J.: Theory of Accelerated Creep and Rupture. Creep and Fracture of Metals at High Temperatures, Her Majesty's Stationery Office (London), 1956, pp. 243-262.
6. Bleakney, H. H.: Intercrystalline Cohesion and the Stress Rupture Test. Proc. ASTM, vol. 47, 1947, pp. 575-589.
7. Jenkins, C. H. M., and Mellor, G. A.: Investigation of the Behavior of Metals Under Deformation at High Temperatures. I - Structural Changes in Mild Steel and Commercial Irons During Creep. Jour. Iron and Steel Inst., vol. 82, 1935, pp. 179-227.
8. Machlin, E. S.: Creep-Rupture by Vacancy Condensation. Jour. Metals, vol. 8, no. 2, sec. 2, Feb. 1956, pp. 106-111.
9. Greenwood, J. N., Miller, D. R., and Suiter, J. W.: Intergranular Cavitation in Stressed Metals. Acta Metall., vol. 2, 1954, pp. 250-258.
10. Smith, G. V.: Properties of Metals at Elevated Temperatures. McGraw-Hill Book Co., Inc., 1950, p. 148.
11. Servi, Italo S., and Grant, Nicholas J.: Creep and Stress Rupture Behavior of Aluminum as a Function of Purity. Trans. AIME, vol. 191, 1951, pp. 909-916.
12. Thielemann, R. H., and Parker, E. R.: Fracture of Steels at Elevated Temperatures after Prolonged Loading. Trans. AIME, vol. 135, 1939, pp. 559-576; discussion, pp. 576-582.
13. Bleakney, H. H.: The Ductility of Metals in Creep-Rupture Tests. Canadian Jour. Tech., vol. 30, 1952, pp. 340-351.
14. Eborall, R.: An Approach to the Problem of Intercrystalline Fracture. Creep and Fracture of Metals at High Temperatures, Her Majesty's Stationery Office (London), 1956, pp. 229-242.
15. Hanson, D., and Wheeler, M. A.: The Deformation of Metals under Prolonged Loading - The Flow and Fracture of Aluminum. Jour. Inst. Metals, vol. 45, no. 1, 1931, pp. 229-257; discussion, pp. 258-264.
16. Seitz, F.: On the Generation of Vacancies by Moving Dislocations. Advances in Phys., vol. 1, no. 1, Jan. 1952, pp. 43-90.
17. Herenguel, J., and Scheidecker, M.: The Strength of Copper Alloys Under a Permanent Mechanical Constraint. Rev. de Métallurgie, t. 48, no. 3, Mar. 1951, pp. 173-181.

18. Balluffi, R. W.: The Supersaturation and Precipitation of Vacancies During Diffusion. *Acta Metall.*, vol. 2, no. 2, Mar. 1954, pp. 194-202.
19. Jenkins, C. H. M., Bucknall, E. H., and Jenkinson, E. A.: The Inter-Relation of Age-Hardening and Creep Performance. Pt. II - The Behavior in Creep of an Alloy Containing 3 Percent Nickel and Silicon in Copper. *Jour. Inst. Metals*, vol. 70, 1944, pp. 57-79.
20. McLean, D.: Grain-Boundary Slip During Creep of Aluminum. *Jour. Inst. Metals*, vol. 81, pt. 6, Feb. 1953, pp. 293-300.
21. Fazan, B., Sherby, O. D., and Dorn, J. E.: Some Observations on Grain Boundary Shearing During Creep. *Jour. Metals*, vol. 6, no. 8, Aug. 1954, pp. 919-922.
22. Dorn, J. E.: Some Fundamental Experiments on High Temperature Creep. *Jour. Mech. and Phys. of Solids*, vol. 3, Jan. 1955, pp. 85-116.
23. Grant, N. J.: Grain Boundary Participation in Creep Deformation and Fracture. *Creep and Fracture of Metals at High Temperatures*, Her Majesty's Stationery Office (London), 1956, pp. 317-330.
24. Resnick, R., and Seigle, L.: Nucleation of Voids in Metals During Diffusion and Creep. *Jour. Metals*, vol. 9, no. 1, sec. 2, Jan. 1957, pp. 87-93.

TABLE I. - DATA FROM CREEP TESTS ON INGOT IRON

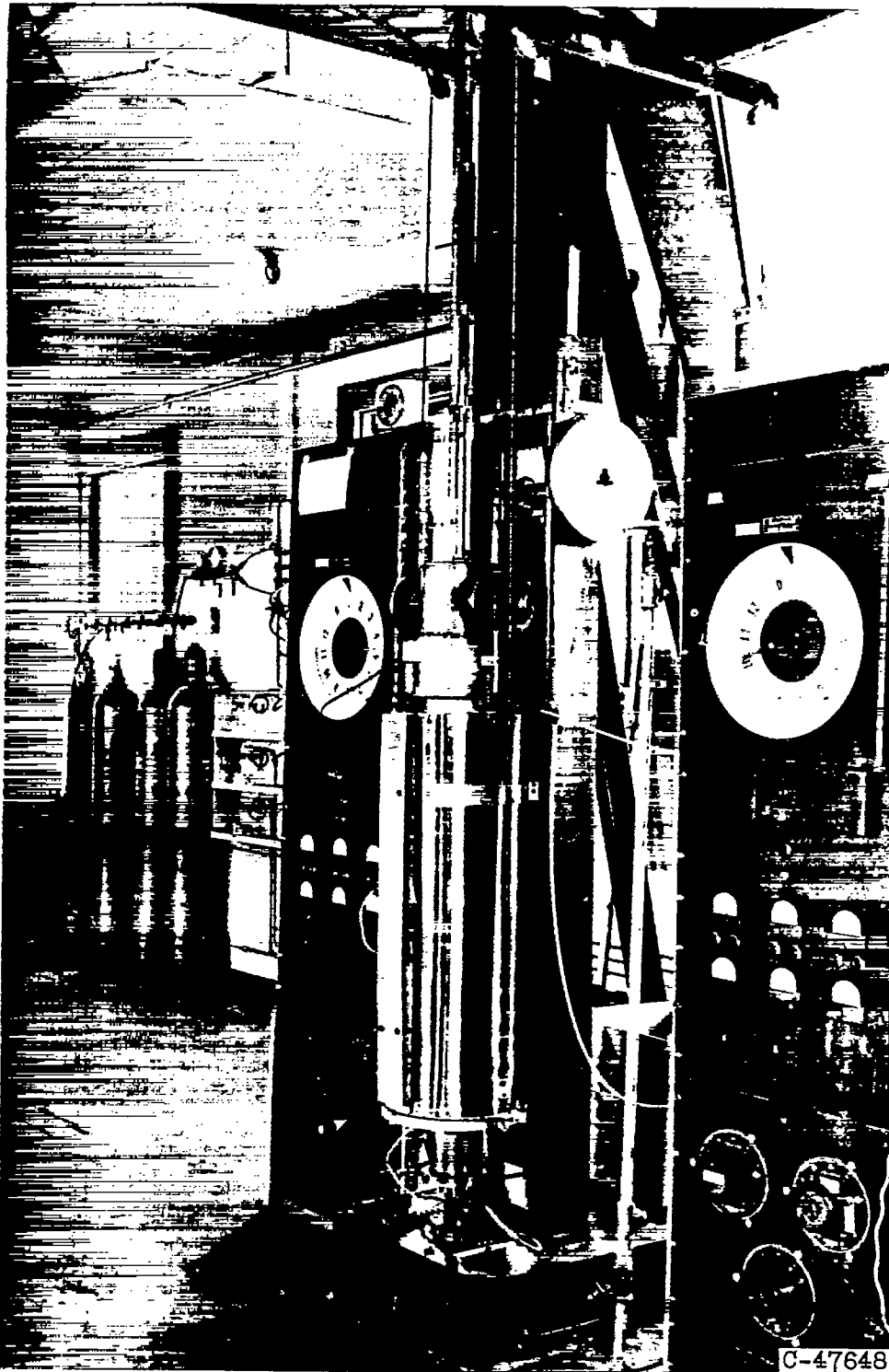
Temperature, °F	Specimen	Stress, psi	Secondary- creep rate, min ⁻¹	Fracture strain, percent	Fracture time, min	Type of fracture (a)
700	B8	25,000	9.2×10^{-4}	31.7	189	T
	B6	25,000	8.7×10^{-4}	25.0	136	T(M)
	B14	22,500	7.9×10^{-5}	30.6	1,180	T
730	C6	25,000	4.6×10^{-3}	21.7	21.75	T
	C7	25,000	5.65×10^{-3}	20.5	15.25	T(M)
	C11	20,000	3.05×10^{-4}	18.35	300	I(M)
750	X6	27,500	5.90×10^{-2}	20.8	1.4	T(M)
	A7	25,000	3.87×10^{-3}	21.7	27	T
	A13	25,000	2.64×10^{-3}	33.3	64	T
	X5	25,000	1.15×10^{-2}	22.6	9.3	T(M)
	T2	25,000	1.22×10^{-2}	29.4	12	T
	A11	22,500	1.24×10^{-3}	27.2	104	T
	B1	20,000	4.6×10^{-4}	19.4	220	I(M)
	X2	20,000	5×10^{-4}	15.7	119.5	I
	T3	20,000	2.38×10^{-4}	15.7	170.8	T
	A15	17,500	1.6×10^{-4}	19.4	1,314	I
	X4	17,500	9.5×10^{-5}	16.1	3,201	I
	775	B3	25,000	3.1×10^{-2}	27.2	4.66
C5		25,000	3.83×10^{-2}	27.2	4	T(M)
C9		25,000	1.26×10^{-2}	28.4	12.25	T
B4		22,500	6.63×10^{-3}	30.5	24	T(M)
C8		22,500	4.27×10^{-3}	29.4	34.66	T
B5		20,000	1.16×10^{-3}	22.0	75	T(M)
C10		20,000	1.24×10^{-3}	20.6	76.3	T(M)
800	A6	25,000	6.9×10^{-2}	15.5	1.25	I(M)
	B2	25,000	7.7×10^{-2}	27.2	2	I(M)
	B7	22,500	1.52×10^{-2}	26.1	8.6	I(M)
	B13	20,000	1.64×10^{-3}	36.1	99.6	T
	X1	17,500	6.0×10^{-4}	15.0	82	I
906	A12	14,000	1.2×10^{-3}	10.5	43.7	I
1020	A4	12,000		9.45	2	I
	A9	6,000	1.05×10^{-4}	7.2	20,200	I
1150	E7	9,000	4.3×10^{-2}	13.9	1.8	I
	E10	8,000	2.7×10^{-2}	13.9	2.5	I
	A1	6,000	1.7×10^{-3}	15.0	53.3	I
	E6	6,000	1.0×10^{-4}	10.5	821	I
	E2	5,000		9.5	1,440	I
	E3	4,000		7.87	756	I
	E9	4,000	1.3×10^{-5}	2.78	1,033	I
	D13	3,500	3.0×10^{-6}	6.12	6,690	I
1250	A2	6,000	1.45×10^{-4}	13.9	4.3	I
	A5	4,000	3.7×10^{-4}	7.2	120	I
1350	D6	5,000		27.2	5.5	I
	E4	4,000	4.1×10^{-3}	25.0	43	I
	E8	4,000	5.6×10^{-3}	23.9	28.5	I
	A3	2,500	6.1×10^{-4}	16.1	182.3	I

aT, transgranular; I, intergranular; (M), mixed.

TABLE II. - SPECIMENS THAT FAILED BOTH TRANSGRANULARLY AND INTERGRANULARLY
AT SAME STRESS AND TEMPERATURE

Temperature, °F	Specimen	Stress, psi	Secondary- creep rate, $\dot{\epsilon}_{\text{sec}}$, min^{-1}	Fracture strain, percent	Fracture time, t_{fr} , min	$\dot{\epsilon}_{\text{sec}} \times t_{\text{fr}}$	Strain at end of second stage, $\epsilon_{\text{end sec}}$	Type of fracture (a)
750	A7	25,000	3.87×10^{-3}	21.7	27	0.105	20.0	T
	X5		1.15×10^{-2}	22.6	9.3	.107	20.3	T(M)
750	T3	20,000	2.38×10^{-4}	15.7	170.8	.0405	14.1	T
	X2		5.0×10^{-4}	15.7	119.5	.0590	14.0	I
775	C9	25,000	1.26×10^{-2}	28.4	12.3	.154	24.8	T
	B3		3.1×10^{-2}	27.2	4.7	.144	25.6	T(M)
775	C8	22,500	4.27×10^{-3}	29.4	34.7	.148	26.3	T
	B4		6.63×10^{-3}	30.5	24	.159	26.8	T(M)

^aT, transgranular; I, intergranular; (M), mixed.



C-47648

Figure 1. - Inert-atmosphere creep testing unit with constant-stress lever arm.

UM-3 back 4936

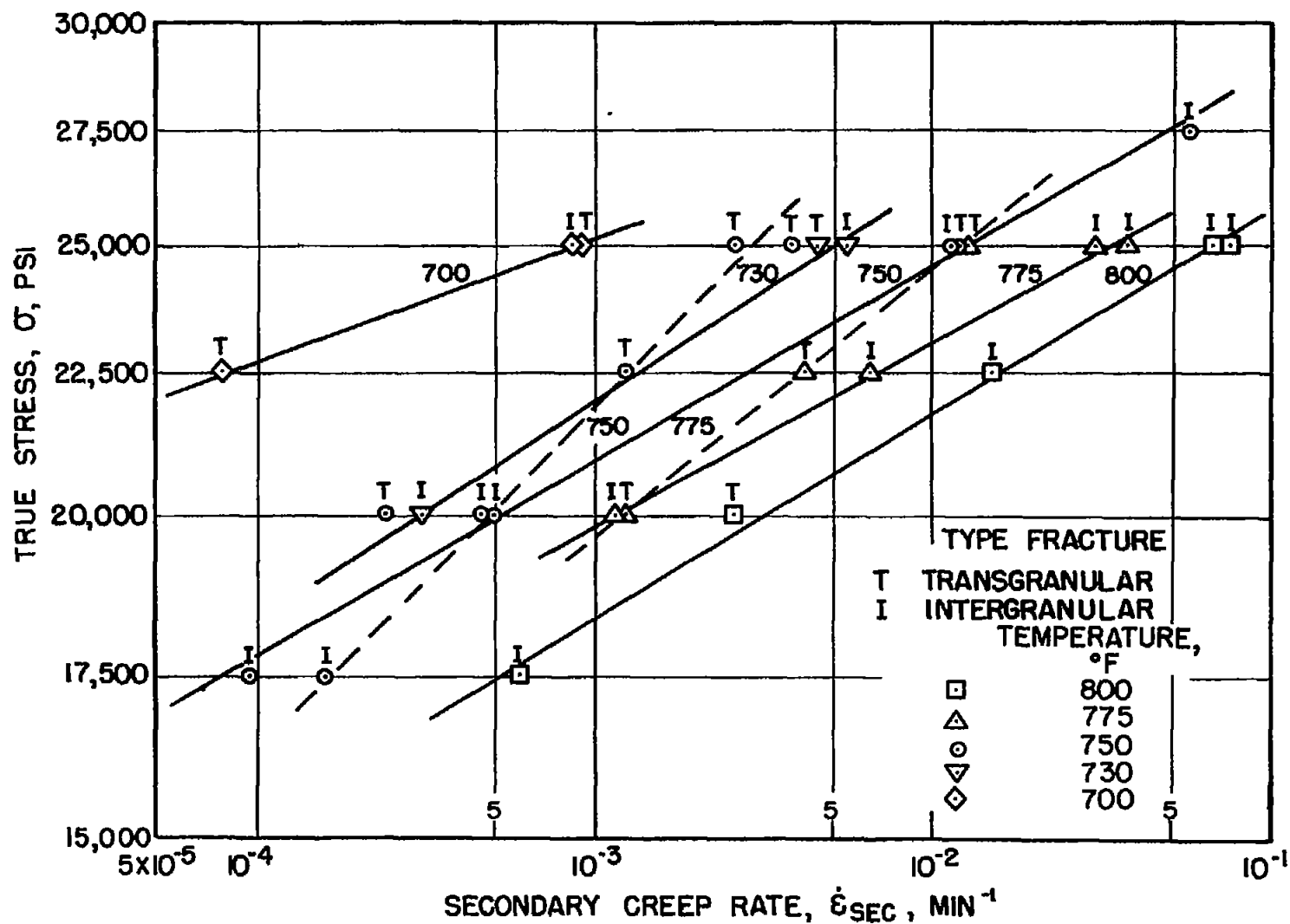


Figure 2. - Plot of log stress against log secondary-creep rate for creep of ingot iron in 700° to 800° F temperature range.

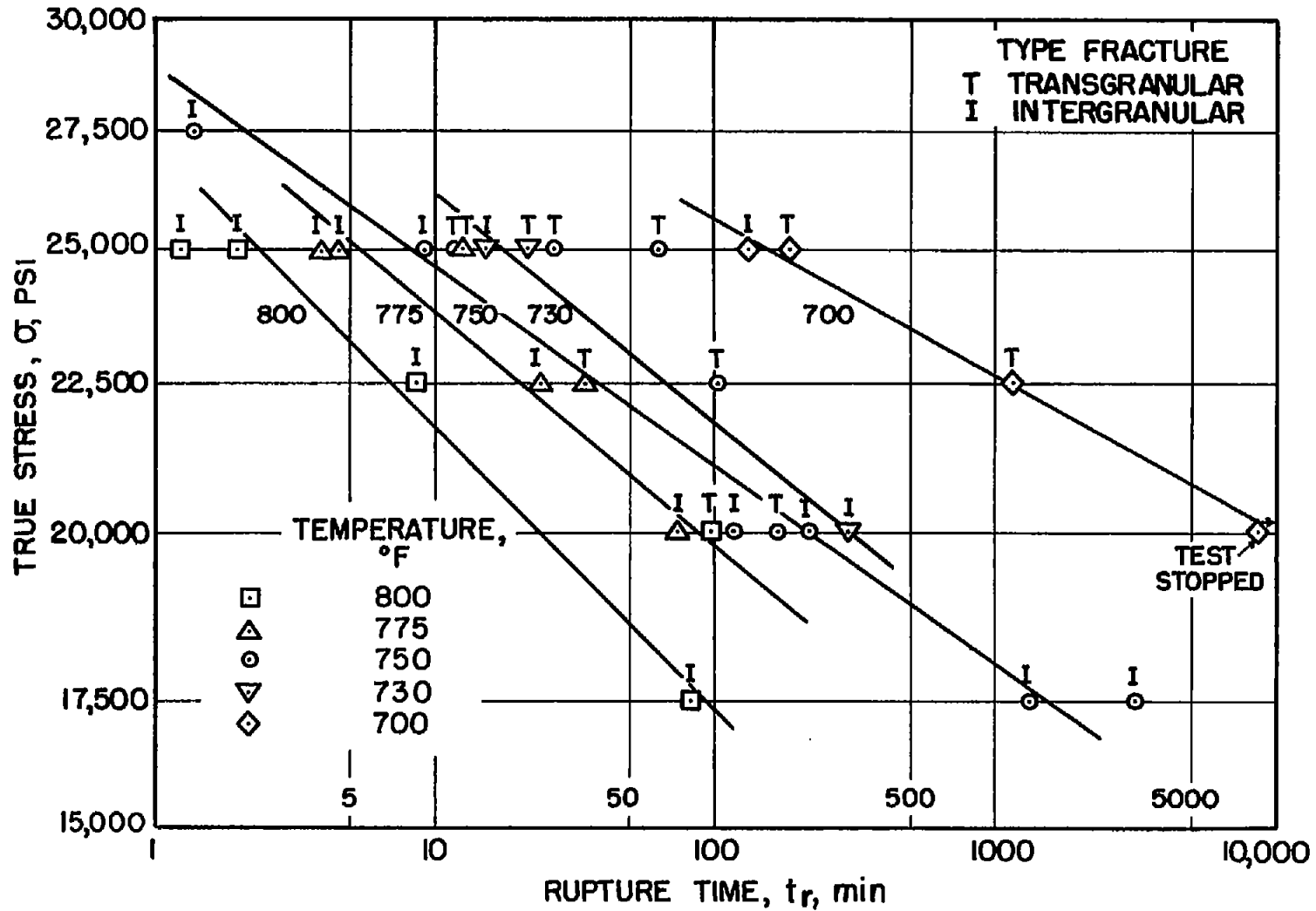
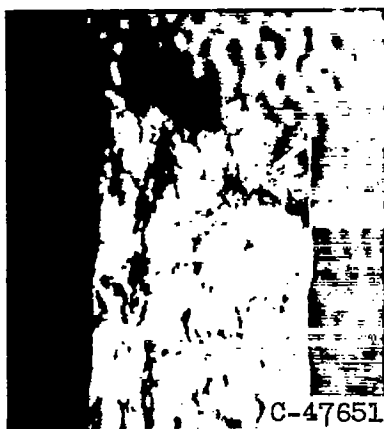


Figure 3. - Plot of log stress against log rupture time for creep of ingot iron in 700° and 800° F temperature range.



Transgranular fracture



Intergranular fracture

Figure 4. - Examples of transgranular and intergranular fractures in coarse-grained ingot iron.

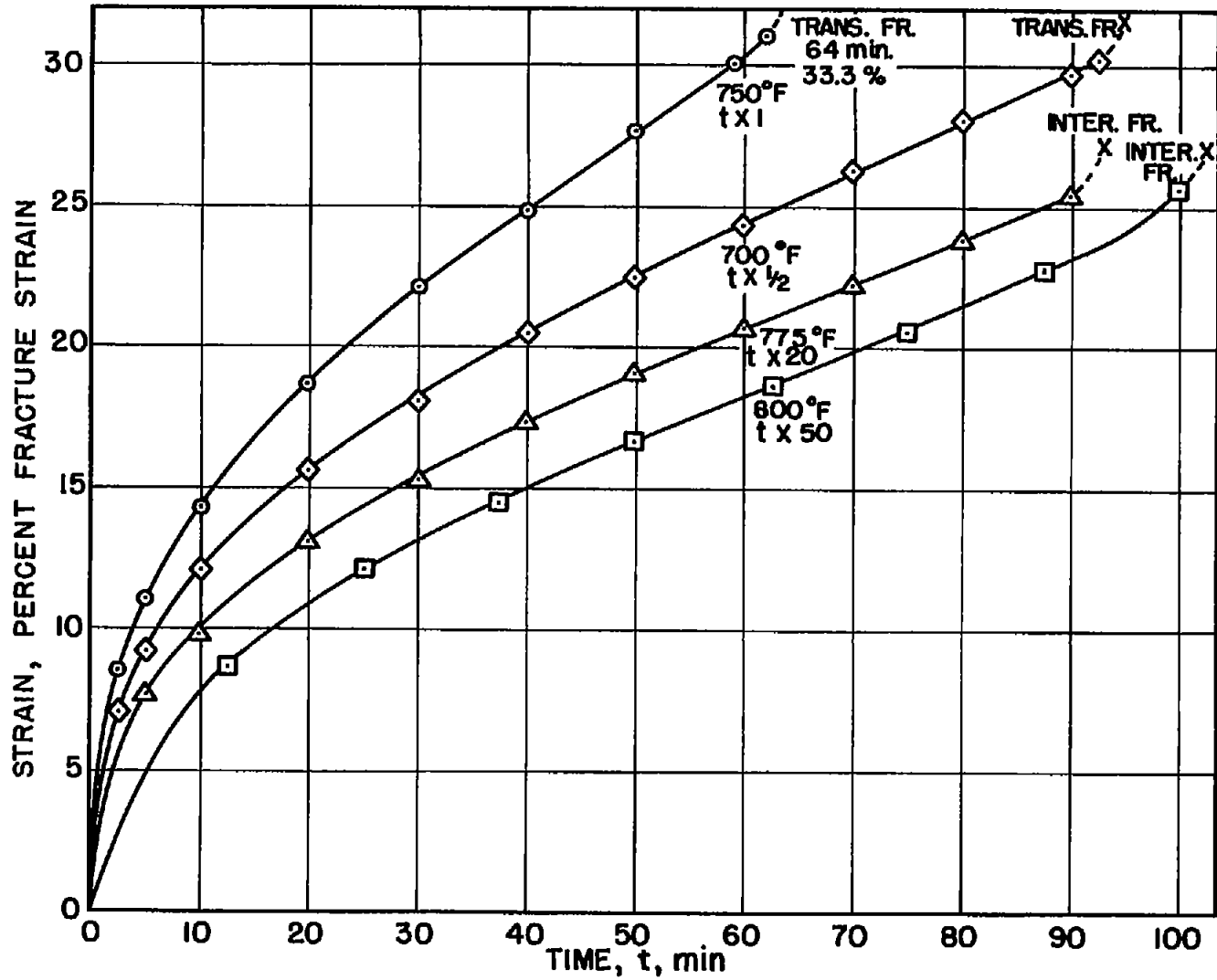


Figure 5. - Typical creep curves for ingot iron in 700° to 800° F temperature range. Stress, 25,000 psi.

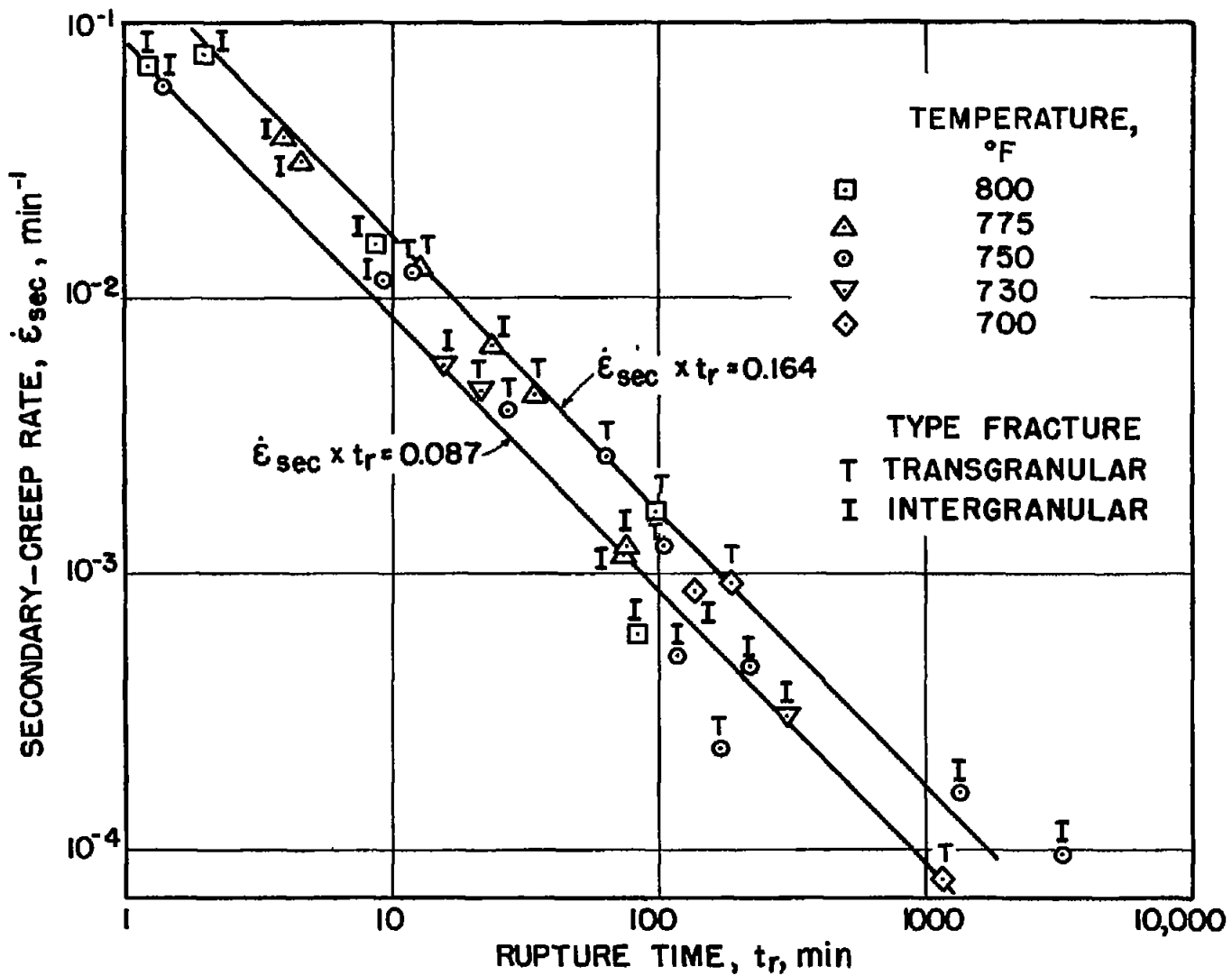


Figure 6. - Plot of log secondary-creep rate against log rupture time for creep of ingot iron in 700° to 800° F temperature range.

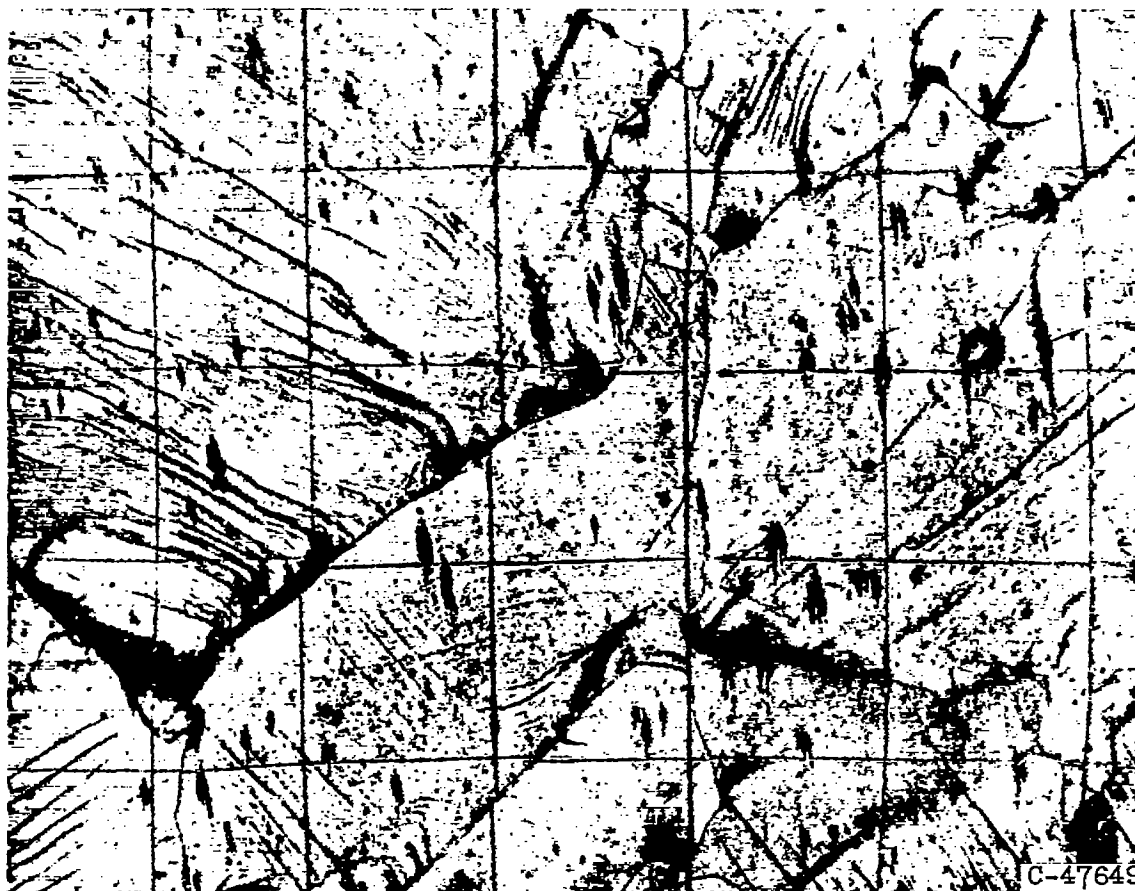


Figure 7. - Grain-boundary shearing during high-temperature creep in ingot iron. Temperature, $1,200^{\circ}$ F; stress, 370,000 psi.



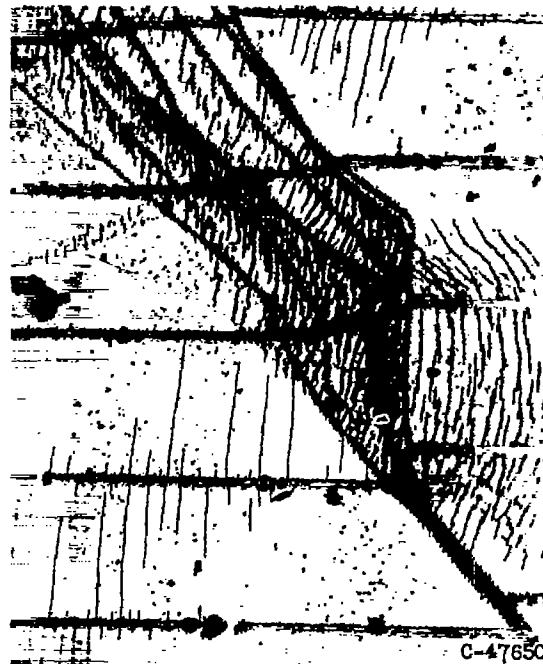
(a) Center of specimen.



(b) Region near fracture.



(c) Area around crack.



(d) Grain-boundary shearing and migration in pure aluminum.

Figure 8. - Distortion of grid lines during creep of ingot iron. Lines emphasized in white for clarity. Temperature, 750° F; stress, 25,000 psi.